Draft version December 6, 2019
Typeset using LaTeX default style in AASTeX63

Is the expansion of the universe accelerating? All signs *still* point to yes

D. Rubin[1,2] and J. Heitlauf[1]

[1] *Department of Physics and Astronomy, University of Hawai'i at Mānoa, Honolulu, Hawai'i 96822*
[2] *E.O. Lawrence Berkeley National Laboratory, 1 Cyclotron Rd., Berkeley, CA, 94720*

Submitted to ApJL

ABSTRACT

Type Ia supernovae (SNe Ia) provided the first strong evidence that the expansion of the universe is accelerating. With SN samples now more than ten times larger than those used for the original discovery and joined by other cosmological probes, this discovery is on even firmer ground. Two recent, related studies (Nielsen et al. 2016 and Colin et al. 2019, hereafter N16 and C19, respectively) have claimed to undermine the statistical significance of the SN Ia constraints. Rubin & Hayden (2016) (hereafter RH16) showed N16 made an incorrect assumption about the distributions of SN Ia light-curve parameters, while C19 also fails to remove the impact of the motion of the solar system from the SN redshifts, interpreting the resulting errors as evidence of a dipole in the deceleration parameter. Building on RH16, we outline the errors C19 makes in their treatment of the data and inference on cosmological parameters. Reproducing the C19 analysis with our proposed fixes, we find that the dipole parameters have little effect on the inferred cosmological parameters. We thus affirm the conclusion of RH16: the evidence for acceleration is secure.

1. INTRODUCTION

The discovery of the accelerated expansion of the universe (Riess et al. 1998; Perlmutter et al. 1999) was originally made through the use of type Ia supernovae (SNe Ia). With measurements of light-curve shape and color, the luminosity can be standardized so that the apparent magnitude can give the distance. Today, multiple cosmological probes combine together to provide a largely consistent picture of the universe on large scales (Planck Collaboration et al. 2018).

A recent study (Colin et al. 2019, hereafter C19) claims that this picture is wrong. They investigate the Joint Light-curve Analysis (JLA) SN Ia compilation (Betoule et al. 2014) and find evidence of a dipole anisotropy in the local deceleration parameter on ~ 100 Mpc scales. C19 claims that this dipole is larger and more statistically significant than the monopole acceleration, for which they find only weak evidence. C19 alleges that this dipole gives rise to falsely strong evidence of the accelerated expansion.

We reevaluate the C19 analysis and find four significant problems, each affecting their results or interpretation.

1. C19's primary analysis makes the plainly incorrect assumption that SN Ia light-curve shape and color distributions are constant as a function of redshift (after selection cuts). That incorrect assumption comes from Nielsen et al. (2016) (hereafter N16), which C19 builds on. However, Rubin & Hayden (2016) (hereafter RH16) has already demonstrated the inaccuracy of this assumption, discussing the need for redshift-dependent observed populations. We summarize that discussion, C19's new (since N16) arguments in favor of this incorrect assumption, and counter C19's objections using statistical significance and physically motivated reasoning. Incorrectly assuming redshift-independent observed distributions has little effect on inferring the dipole parameters, but causes large biases in the monopole cosmological parameters. The net result of these biases weakens a portion of the standardization of distant SNe, moving these SNe brighter and thus biasing the inferred cosmology towards less acceleration.

Corresponding author: David Rubin
drubin@hawaii.edu

2. Shockingly, C19 use *heliocentric* redshifts to compute their comoving model distances, leaving the well-established motion of the solar system with respect to the cosmic microwave background to imprint on the SN redshifts. They further use SNe as close as redshift 0.01, where the decision to use heliocentric or CMB redshifts affects the distance modulus at up to $(5/\log(10))(370\ \mathrm{km/s})/(0.01\ c) \approx \pm 0.27$ magnitudes. This distance modulus difference is far dominant over per-SN distance uncertainty and is correlated across the sky. In addition to using heliocentric redshift, C19 removed the peculiar-velocity covariance terms from the JLA distance-modulus-uncertainty covariance matrix. This is in keeping with the spirit of using heliocentric redshifts, as C19 did not apply a peculiar-velocity model. However the removal of these covariance terms has a significant impact. When the full JLA peculiar-velocity covariance matrix is included in the analysis, we find no statistically significant anisotropy at 2σ, *even when using C19's preferred heliocentric redshift.* We show that these two related decisions are the primary driver of C19's claimed dipole anisotropy.

   C19's justification of the heliocentric choice is weak, citing evidence that bulk flows may exist on larger-than-expected scales. However, the choice to work in heliocentric redshifts is arbitrary; C19 shows no evidence that the heliocentric frame is closer to the average reference frame of nearby SN hosts than the CMB frame, let alone that it is better than employing the CMB frame plus corrections for known peculiar velocities (as the JLA analysis did). If the authors of C19 are concerned about the impact of peculiar velocities, then it makes very little sense to remove the peculiar-velocity-uncertainty covariances from the analysis.

3. C19 calls out the hemispheric imbalance of surveys included in the JLA compilation; most SNe included are from Northern-hemisphere telescopes. However, C19 completely ignores consistent cosmological results from SNe published more recently than JLA that have been obtained with Southern-hemisphere telescopes (Carnegie Supernova Project Krisciunas et al. 2017 and the Dark Energy Survey Abbott et al. 2019). C19 also ignores their own analysis's failure to find a strong correlation between the dipole term and the monopole term (their Figure 3), which suggests that choice of hemisphere does not affect the JLA analysis.

4. The C19 preferred model for the dipole anisotropy (which they use for all their quoted results) is pathological when modeling an isotropic universe (with no dipole). As the C19 dipole falls off exponentially with redshift, a model with no observable dipole can be made either by setting the dipole term to zero, or by setting the dipole term to any positive or negative value and the scale factor of the exponential to a value much smaller than the SN redshifts. We find that we must restrict the range of S around the best-fit range found by C19 to achieve reasonable frequentist coverage (e.g., 68% of the time, the true answer is in the 68% credible interval). This difference could be the source of the non-Gaussian behavior of their contours as the dipole approaches zero (their Figure 3), a feature that we do not see in our analysis.

Our response is structured as follows. Section 2 discusses our version of the C19 analysis, based heavily on the work of RH16. Section 3 shows our cosmological constraints. We run analyses with heliocentric redshifts, CMB-centric redshifts, and CMB-centric redshifts with the peculiar-velocity model JLA used (Hudson et al. 2004; Conley et al. 2011) removed. We further investigate the impact of the peculiar-velocity covariances that C19 removed. Section 4 summarizes and concludes.

2. ANALYSIS AND REANALYSIS

This section begins by reviewing kinematic parameters and outlining the C19 cosmological model (Section 2.1). Section 2.2 describes our implementation of the analysis. Finally, Section 2.3 discusses the importance of allowing the observed SN population distributions (after selection) to change with redshift, and dismantles the C19 claim that constant population distributions are preferred.

2.1. *Kinematic Parameters*

The origin of the kinematic parameters is a series expansion of the scale factor $a(t)$ around the present time $t = t_0$:

$$a(t) = a_0 \left[1 + H_0(t - t_0) - \frac{1}{2!} q_0 H_0^2 (t - t_0)^2 + \frac{1}{3!} j_0 H_0^3 (t - t_0)^3 + \mathcal{O}([t - t_0]^4) \right] . \tag{1}$$

a_0 is frequently defined to be 1. H_0 is the Hubble constant (or the Hubble parameter evaluated at $t = t_0$), given by

$$H_0 \equiv \frac{\dot{a}(t)}{a(t)}|_{t=t_0} . \tag{2}$$

q_0 is the deceleration parameter and is given by

$$q_0 \equiv -\frac{\ddot{a}(t)a(t)}{\dot{a}^2(t)}|_{t=t_0} \; ; \tag{3}$$

the negative sign is a historical convention from when the expansion of the universe was assumed to be decelerating, making $\ddot{a}(t)$ negative. j_0 is the jerk parameter and is given by

$$j_0 \equiv \frac{\dddot{a}(t)a^2(t)}{\dot{a}^3(t)}|_{t=t_0} \; . \tag{4}$$

C19 follows Visser (2004) in using the following series expansion for luminosity distance

$$d_L(z) = \frac{cz}{H_0}\left[1 + \frac{1}{2}(1-q_0)z - \frac{1}{6}(1 - q_0 - 3q_0^2 + j_0 - \Omega_k)z^2\right] \; . \tag{5}$$

As $d_L = (1+z_{\mathrm{heliocentric}})$ times comoving distance, we slightly modify this expression so that it scales as $(1+z_{\mathrm{heliocentric}})$:

$$d_L(z,\; z_{\mathrm{heliocentric}}) = \frac{1+z_{\mathrm{heliocentric}}}{1+z}\frac{cz}{H_0}\left[1 + \frac{1}{2}(1-q_0)z - \frac{1}{6}(1 - q_0 - 3q_0^2 + j_0 - \Omega_k)z^2\right] \; , \tag{6}$$

where z is heliocentric, CMB-centric, or CMB-centric with peculiar-velocity corrections. We form the distance modulus as

$$\mu(z,\; z_{\mathrm{heliocentric}}) = 5\log_{10}\left[\frac{d_L(z,\; z_{\mathrm{heliocentric}})}{10 \text{ parsec}}\right] \; . \tag{7}$$

The C19 model separates q_0 into a monopole q_{0m} and a dipole q_{0d} which C19 points in the direction of the CMB dipole ($\vec{n}_{\mathrm{CMB}}$) in the their baseline analysis.

$$q_0(z_{\mathrm{SN}}, \vec{n}_{\mathrm{SN}}) = q_{0m} + q_{0d}(\vec{n}_{\mathrm{SN}} \cdot \vec{n}_{\mathrm{CMB}})\; e^{-z_{\mathrm{SN}/S}} \tag{8}$$

S is the scale (in redshift) over which the dipole term falls off.

2.2. *Parameter Inference*

As noted above, much of our analysis follows RH16, including implemeting the model in Stan (Carpenter et al. 2017) with Pystan (https://doi.org/10.5281/zenodo.598257). We use 40 chains, each of which draws 1,000 samples after 1,000 discarded burn-in samples. We publish our code as an update to the original RH16 analysis.[1] We (and C19) use a simple Bayesian hierarchical model for linear standardization of SNe Ia (c.f., Gull 1989; March et al. 2011). We treat all parameters in a Bayesian framework, while C19 uses frequentist statistics for the cosmological parameters (and other global parameters). The posteriors on these parameters are relatively Gaussian, so this is not a significant difference.

As discussed in Section 1, the model in Equation 8 has pathologies. A model with no dipole can either be made by setting q_{0d} to zero, or q_{0d} to any positive or negative number with S made much smaller than the minimum SN redshift (0.01). For ease of comparison to C19, we use their model for our results. To ensure good frequentist coverage of our inference (especially on q_{0d}, which is better constrained than S), we use simulated-data testing. We use the actual coordinates and redshifts of the nearby SNe ($z < 0.15$) in JLA, and simulate data with $q_{0d} = 8$ (as in C19) and $q_{0d} = 0$. Running many simulations, we find that we need to restrict S to give reasonable frequentist coverage for the inference. We restrict S to the range 0.02–0.03, matching the range of S values from C19 when q_{0m}, q_{0d}, and S are simultaneously inferred.

2.3. *Population Distributions*

To illustrate the necessity of modeling the changes in the observed light-curve-parameter distributions with redshift, we simulate a very simple survey with just color and magnitude. The intrinsic color population is assumed to be Gaussian with width 0.1 magnitudes and mean 0 (constant in redshift). We generate redshifts with $P(z) \propto z^2$

[1] https://github.com/rubind/SimpleBayesJLA

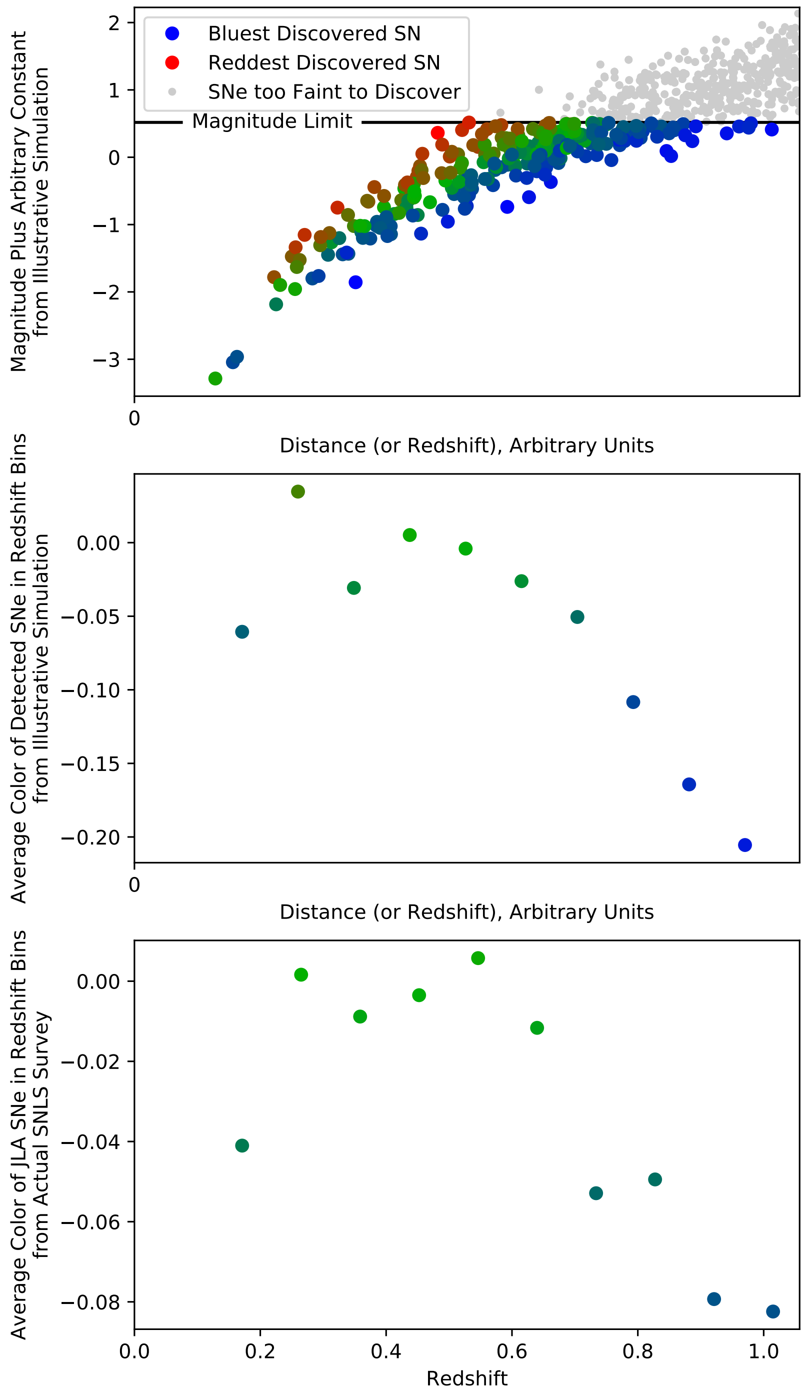

Figure 1. Illustration of the interaction of observed light-curve-parameter distributions and selection effects. We run a simple simulated survey containing only color and magnitude. This simulation assumes a distance modulus of $5\log_{10}$(redshift) and a constant volumetric rate ($P(z) \propto z^2$), and is thus scale-invariant. In other words, both the redshift/distance are in arbitrary units, and the magnitudes are only defined up to an additive constant. The **top panel** shows magnitude plotted against true distance (or redshift); the detected SNe (brighter than a cutoff magnitude) are plotted from blue to red according to their color. The SNe fainter than the cutoff magnitude are shown in light gray. This plot shows that magnitude correlates with both color and distance, and thus bluer SNe can be seen to much greater distances than redder SNe. The **middle panel** shows average color of detected simulated SNe in bins. A clear trend towards detecting bluer SNe with greater distance is seen. The **bottom panel** shows binned color vs. redshift for the real SNLS survey (see also RH16 Figure 1). The trend is qualitatively similar but quantitatively different (as a number of real-world effects were ignored in this simple simulation). This simple simulation shows that there is a strong expectation that the average color of detected SNe should vary significantly with redshift for magnitude-limited samples, even in the case where SNe have the same intrinsic population distribution at all redshifts.

(following a constant volumetric rate), then construct magnitudes using $5\log_{10}(\text{distance}) + 3.1$ color + arbitrary constant, assuming distance $\propto$ redshift. For illustrative purposes, we apply a hard magnitude limit, in contrast to actual selection probabilities, which are smooth with magnitude (e.g., Perrett et al. 2010). Figure 1 shows the results of this simulation and qualitative agreement with the actual color trend with redshift in the SuperNova Legacy Survey in the JLA analysis.

RH16 introduced 12 additional parameters: for the nearby SNe, the Sloan Digital Sky Survey SNe, and the SuperNova Legacy Survey SNe, mean color and light-curve shape (after selection) are modeled as linear functions in redshift. Of course, the averages are not quite linear with redshift, but this is close enough over most of the redshift range of most of the SNe in each survey that more redshift-flexible models do not significantly change the cosmological inference (as noted in RH16).[2] C19 criticize the inclusion of these 12 additional parameters on three grounds, all of which are demonstrably false.

C19 claims that the additional fit parameters are a posteriori, in other words that these parameters were deliberately added by RH16 to the N16 analysis to recover the concordance cosmology. However, the importance of redshift-dependent color population distributions was well established much earlier than the N16 paper, e.g. in Wood-Vasey et al. (2007); Kessler et al. (2009); Karpenka (2015); Rubin et al. (2015). The intrinsic light-curve shape population distribution is expected to be redshift-dependent as well, as there is a correlation between light-curve shape and host-galaxy properties (Hamuy et al. 1995).

C19 further claims that the additional parameters are not justified by the Bayesian information criterion (Schwarz 1978), a frequently used method that penalizes -2 log(likelihood) with $k\log(n)$ for k parameters and n observations. As discussed above, we have a strong expectation that the observed light-curve population distributions should be redshift dependent, negating this objection to the 12 additional parameters of RH16 even if these parameters were not favored by the Bayesian information criterion. The C19 implementation of the RH16 model gives a -2 log(likelihood) that ranges from -298 to -332, depending on other fit parameters. The C19 constant-populations-in-redshift model gives a -2 log(likelihood) that ranges from -190 to -217. The Bayesian information criterion relative penalty for 740 measurements (as there are 740 SNe in the JLA compilation) and 12 additional parameters is $12\log(740) = 79$, much less than the -2 log(likelihood) difference. Thus C19's own values show that the RH16 model is actually preferred *using the information criterion that C19 claims to be using.*

Finally, C19 criticizes RH16 for focusing on the light-curve shape and color parameters to the exclusion of magnitude. This claim is also false, as described in RH16. As part of the JLA analysis, Betoule et al. (2014) included simulations of the impact of selection effects on each SN sample, removed its impact on magnitude, and propagated the uncertainties into the covariance matrix (much of this work was built on Conley et al. 2011). This bias is different from the deficient standardization that one gets from ignoring the redshift dependence of the population distributions, which is due to biasing the inferred latent values of light-curve shape and color. Intrinsic magnitude differences with redshift are controlled for by matching SNe in bins of host-galaxy stellar mass (as an easier-to-measure proxy for SN progenitor age or metallicity). In any case, the systematic uncertainties due to such effects are a small fraction of the signature of acceleration in the SN Ia data, and a fraction of the bias caused by ignoring the redshift dependence of the population distributions.

3. COSMOLOGICAL CONSTRAINTS

Figure 2 shows the 68.3% credible regions and intervals for the cosmological parameters. This figure shows constraints for three cases: heliocentric redshifts, CMB-centric redshifts, and CMB-centric redshifts with peculiar-velocity corrections. To match C19, we remove the peculiar-velocity covariances from the JLA covariance matrix. We see that the choice of redshift frame mostly affects q_{0d}. Figure 3 shows the same cosmological constraints with the JLA peculiar-velocity covariance matrix included. In contrast to the results without this part of the covariance matrix, q_{0d} is consistent with zero at 2σ for all three types of redshifts.

It is worth briefly discussing the interpretation of series expansions (kinematic expansions) of the expansion history (Equation 1) to understand the strong correlation between q_0 and $j_0 - \Omega_k$. Frequently, we speak imprecisely about measuring H_0, q_0, or j_0 from SNe Ia (possibly combined with other probes). However, SNe measure distances at finite redshift and thus effectively measure these quantities at nonzero (but low) redshift. For example, the (statistically disfavored) not-currently-accelerating (q_0 forced to 0) models of C19 (in Table A.1) have $j_0 - \Omega_k \sim -1.35$, and so

[2] An even better approach is to model both the selection process and the intrinsic population distribution as a function of SN sample and/or redshift. This can be done either as a simultaneous Bayesian model (Rubin et al. 2015) or with simulations (Scolnic & Kessler 2016).

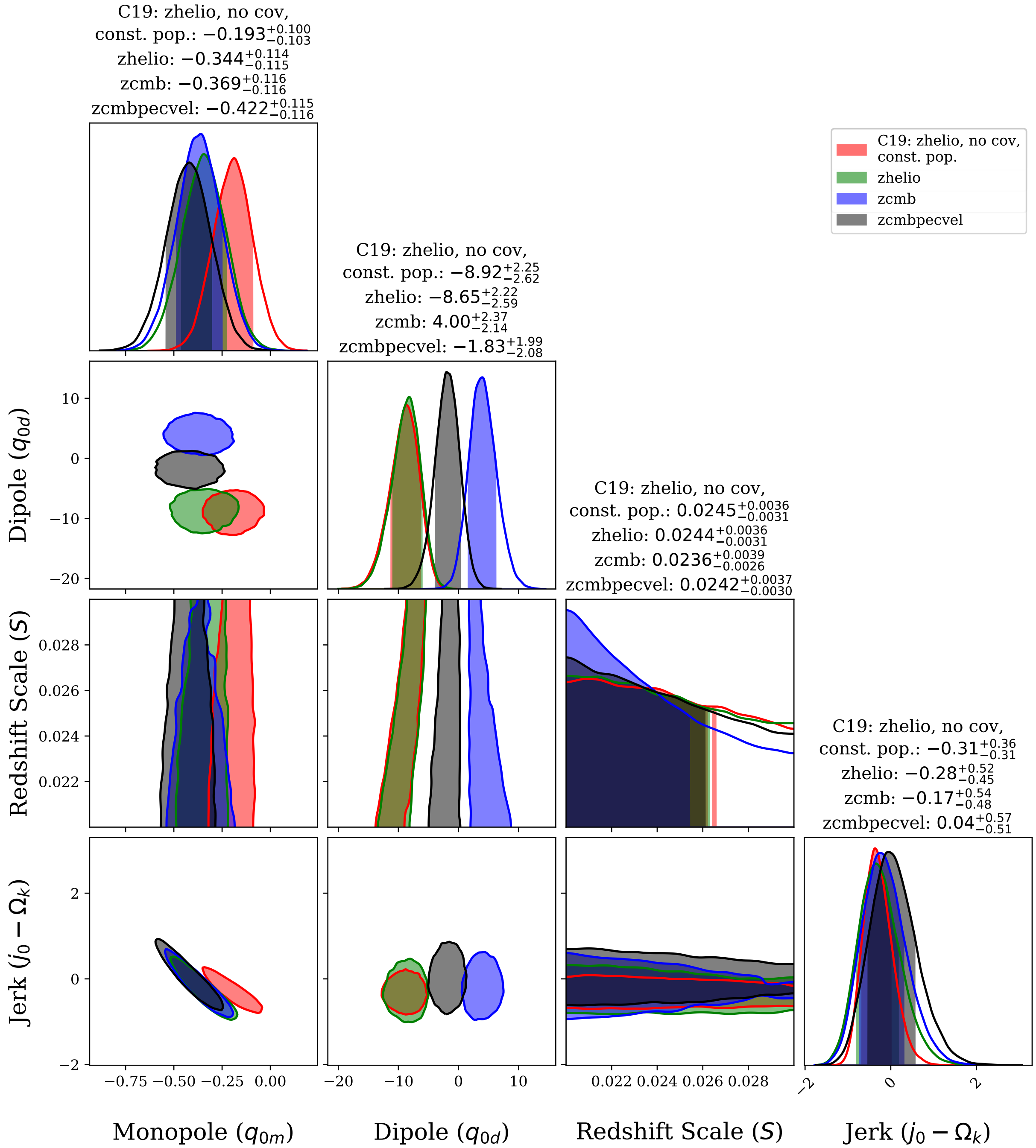

Figure 2. 68.3% credible regions and intervals for cosmological parameters. We show the results from the C19 assumptions (heliocentric redshifts, no peculiar-velocity-uncertainty covariances, and redshift-independent observed light-curve population distributions) in red. For our assumptions, we use all three considered redshifts: heliocentric (green), CMB-centric (blue), and CMB-centric with peculiar-velocity corrections (black), all of which have the RH16 redshift-dependent population model. We remove the peculiar-velocity covariances from the JLA covariance matrix to match C19. The cosmological parameter impacted the most by the redshift variants is q_{0d}. In particular, we see moderate evidence for a non-zero q_{0d} dipole when heliocentric redshifts are used, but this evidence drops to $< 2\sigma$ for the other redshifts. The results using C19 assumptions are significantly offset due to their population model.

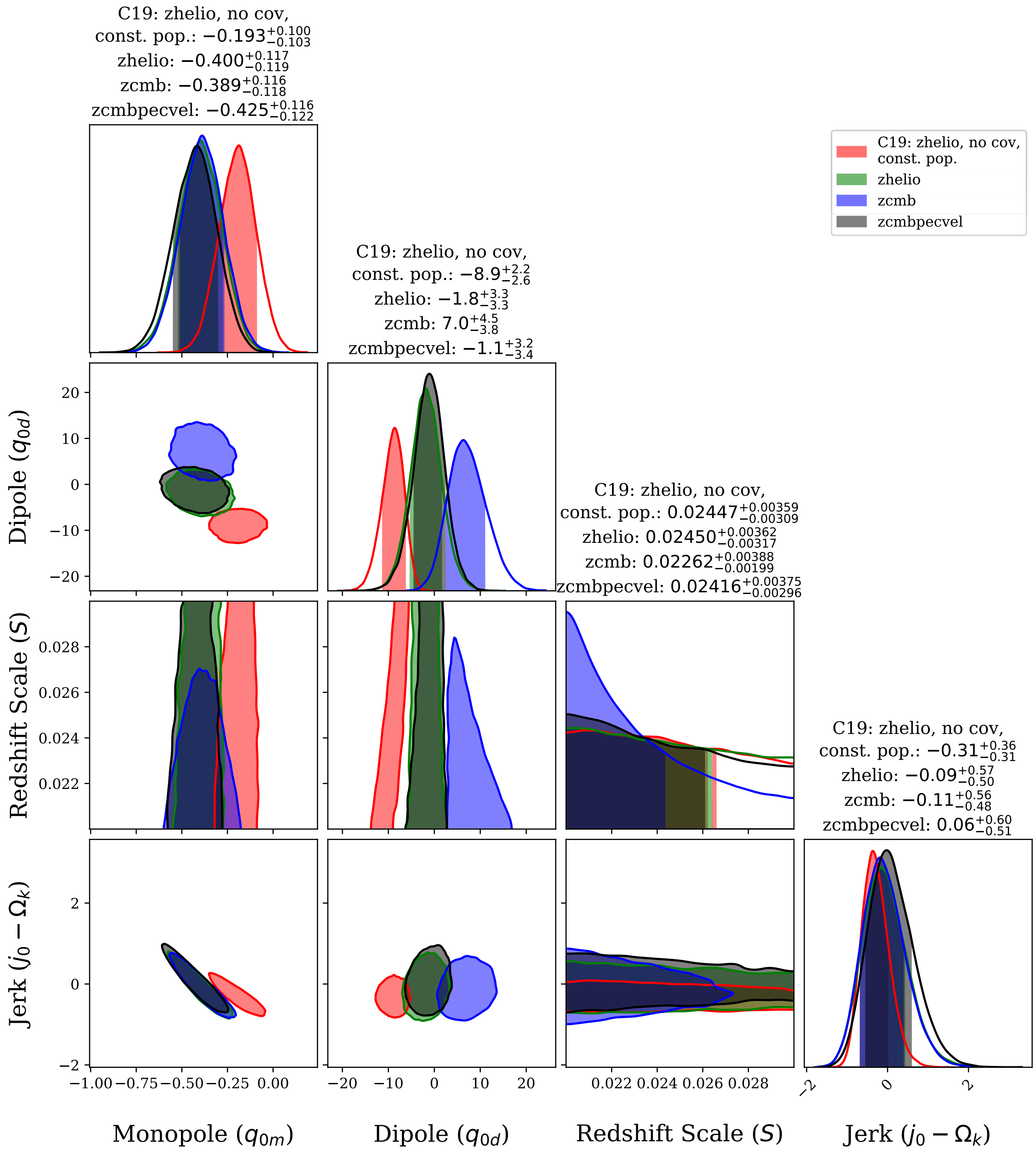

Figure 3. 68.3% credible regions and intervals for cosmological parameters. We show the results from the C19 assumptions (heliocentric redshifts, no peculiar-velocity-uncertainty covariances, and redshift-independent observed light-curve population distributions) in red. For our assumptions, we use all three considered redshifts: heliocentric (green), CMB-centric (blue), and CMB-centric with peculiar-velocity corrections (black), all of which have the RH16 redshift-dependent population model. Unlike Figure 2, the peculiar-velocity-uncertainty covariances are included, as they were in the JLA analysis. In contrast to the results without the peculiar-velocity covariances, all of our cosmological results are consistent, with only a modest difference in q_{0d}. The results using C19 assumptions are again significantly offset.

would have experienced several Gyrs of acceleration in the recent past ($j_0 < 0$), even though the acceleration goes to zero today. See RH16 for a discussion of $q_0/j_0 - \Omega_k$ JLA constraints using other (physical) models.

4. CONCLUSION

This work reimplements the C19 cosmological analysis to investigate their claims of a dipole term in the deceleration parameter (q_{0d}) and a statistically weak monopole (q_{0m}).

We show that the weak monopole finding is identical to the finding from the related N16 analysis, which was rebutted by RH16 for their incorrect use of constant-in-redshift SN populations (after selection). We find the same criticism still applies, and counter the C19 arguments against RH16, including finding an apparent miscalculation in the C19 Bayesian information criterion.

We find that the C19 (3.9σ) result of a significant q_{0d} depends strongly on both failing to remove our motion from the redshifts of SNe (that is, working in the heliocentric frame) and failing to include the JLA peculiar-velocity covariances. Changing either of these brings the evidence for a dipole below 2σ. Despite the inclusion of the dipole term, we see virtually the same constraints on q_{0m} as RH16 saw on q_0 when using the same type of redshift model and using the same covariance matrix. We thus conclude that concerns over the value of q_{0d} have little effect on the strength of the evidence for acceleration.

ACKNOWLEDGMENTS

The technical support and advanced computing resources from the University of Hawaii Information Technology Services Cyberinfrastructure are gratefully acknowledged. We thank Greg Aldering, Benjamin Rose, and Brian Hayden for careful feedback.

Software: Matplotlib (Hunter 2007), Numpy (van der Walt et al. 2011), pystan (https://doi.org/10.5281/zenodo.598257), Python, SciPy (Jones et al. 2001), Stan (Carpenter et al. 2017)

REFERENCES

Abbott, T. M. C., Allam, S., Andersen, P., et al. 2019, ApJL, 872, L30

Betoule, M., Kessler, R., Guy, J., et al. 2014, A&A, 568, A22

Carpenter, B., Gelman, A., Hoffman, M., et al. 2017, Journal of Statistical Software, Articles, 76, 1. https://www.jstatsoft.org/v076/i01

Colin, J., Mohayaee, R., Rameez, M., & Sarkar, S. 2019, A&A, 631, L13

Conley, A., Guy, J., Sullivan, M., et al. 2011, ApJS, 192, 1

Gull, S. F. 1989, Bayesian Data Analysis: Straight-line fitting, ed. J. Skilling (Dordrecht: Springer Netherlands), 511–518. https://doi.org/10.1007/978-94-015-7860-8_55

Hamuy, M., Phillips, M. M., Maza, J., et al. 1995, AJ, 109, 1

Hudson, M. J., Smith, R. J., Lucey, J. R., & Branchini, E. 2004, MNRAS, 352, 61

Hunter, J. D. 2007, Computing in Science & Engineering, 9, 90

Jones, E., Oliphant, T., Peterson, P., et al. 2001, SciPy: Open Source Scientific Tools for Python, ,

Karpenka, N. V. 2015, The supernova cosmology cookbook: Bayesian numerical recipes, , , arXiv:1503.03844

Kessler, R., Becker, A. C., Cinabro, D., et al. 2009, ApJS, 185, 32

Krisciunas, K., Contreras, C., Burns, C. R., et al. 2017, AJ, 154, 211

March, M. C., Trotta, R., Berkes, P., Starkman, G. D., & Vaudrevange, P. M. 2011, Monthly Notices of the Royal Astronomical Society, 418, 2308. https://onlinelibrary.wiley.com/doi/abs/10.1111/j.1365-2966.2011.19584.x

Nielsen, J. T., Guffanti, A., & Sarkar, S. 2016, Scientific Reports, 6, 35596

Perlmutter, S., Aldering, G., Goldhaber, G., et al. 1999, ApJ, 517, 565

Perrett, K., Balam, D., Sullivan, M., et al. 2010, AJ, 140, 518

Planck Collaboration, Aghanim, N., Akrami, Y., et al. 2018, arXiv e-prints, arXiv:1807.06209

Riess, A. G., Filippenko, A. V., Challis, P., et al. 1998, AJ, 116, 1009

Rubin, D., & Hayden, B. 2016, ApJL, 833, L30

Rubin, D., Aldering, G., Barbary, K., et al. 2015, ApJ, 813, 137

Schwarz, G. 1978, Ann. Statist., 6, 461. https://doi.org/10.1214/aos/1176344136

Scolnic, D., & Kessler, R. 2016, ApJL, 822, L35

van der Walt, S., Colbert, S. C., & Varoquaux, G. 2011, Computing in Science & Engineering, 13, 22

Visser, M. 2004, Classical and Quantum Gravity, 21, 2603

Wood-Vasey, W. M., Miknaitis, G., Stubbs, C. W., et al. 2007, ApJ, 666, 694